Virologica Sinica 38 (2023) 380–386

Contents lists available at ScienceDirect

Virologica Sinica

journal homepage: www.keaipublishing.com/en/journals/virologica-sinica
www.virosin.org

Research Article

Deletion of the first glycosylation site promotes Lassa virus glycoprotein-mediated membrane fusion

Siqi Dong [a,b,1], Wenting Mao [a,b,1], Yang Liu [a], Xiaoying Jia [a,b], Yueli Zhang [a,c], Minmin Zhou [a,b], Yuxia Hou [a,b], Gengfu Xiao [a,b], Wei Wang [a,b,*]

[a] State Key Laboratory of Virology, Wuhan Institute of Virology, Center for Biosafety Mega-Science, Chinese Academy of Sciences, Wuhan, 430207, China
[b] University of the Chinese Academy of Sciences, Beijing, 100049, China
[c] College of Pharmacy and State Key Laboratory of Medicinal Chemical Biology, Nankai University, Tianjin, 300071, China

ARTICLE INFO

Keywords:
Lassa virus (LASV)
Glycoprotein complex (GPC)
Glycosylation site
Membrane fusion

ABSTRACT

The Lassa virus (LASV) is endemic in West Africa and causes severe hemorrhagic Lassa fever in humans. The glycoprotein complex (GPC) of LASV is highly glycosylation-modified, with 11 N-glycosylation sites. All 11 N-linked glycan chains play critical roles in GPC cleavage, folding, receptor binding, membrane fusion, and immune evasion. In this study, we focused on the first glycosylation site because its deletion mutant (N79Q) results in an unexpected enhanced membrane fusion, whereas it exerts little effect on GPC expression, cleavage, and receptor binding. Meanwhile, the pseudotype virus bearing GPC_{N79Q} was more sensitive to the neutralizing antibody 37.7H and was attenuated in virulence. Exploring the biological functions of the key glycosylation site on LASV GPC will help elucidate the mechanism of LASV infection and provide strategies for the development of attenuated vaccines against LASV infection.

1. Introduction

Lassa virus (LASV) is a negative-sense, bi-segmented RNA virus that belongs to the genus *Mammarenavirus* in the *Arenaviridae* family (Kuhn et al., 2021). Mammarenaviruses consist of 35 unique species and are divided into New World (NW) and Old World (OW) mammarenaviruses mainly based on viral genetics, serology, antigenic properties, and geographical relationships (Kuhn et al., 2021; Nunberg and York, 2012). LASV belongs to the OW family, which also contains the prototype mammarenavirus lymphocytic choriomeningitis virus (LCMV) and the closely related Mopeia virus (MOPV). The natural host of LASV is *Mastomys natalensis*. LASV is commonly transmitted to humans through ingestion or inhalation (Lukashevich and Torre, 2021; Lo Iacono et al., 2015; McCormick et al., 1987). LASV infection causes an acute infectious hemorrhagic disease called Lassa fever. Approximately 300,000–500,000 people are infected with LASV annually, and the mortality of hospitalized patients ranges between 20% and 70% (Houlihan and Behrens, 2017). As of October 9, 2022, there were 937 confirmed cases and 173 deaths in Nigeria (https://ncdc.gov.ng/). Currently, there is no drug or vaccine for the treatment of Lassa fever approved by the Food and Drug Administration.

The envelope glycoprotein complex (GPC) of LASV is a type I fusion protein and is anchored as a homotrimer on the surface of the virus. Each GPC monomer contains a stable signal peptide (SSP), receptor-binding subunit GP1, and membrane fusion subunit GP2 (Lenz et al., 2001; Eichler et al., 2003). LASV GPC is a heavily glycosylation-modified protein containing 11 N-glycosylation sites (Asn-X-Thr/Ser, where X is any amino acid except proline), 7 of which are located in GP1 and 4 in GP2 (Hastie et al., 2017; Wang et al., 2016).

The roles of the individual glycosylation site in arenavirus GPC have been well studied. Some glycosylation site deletion mutants disrupt the processing and cell membrane surface transport of GPC (Eichler et al., 2006; Zhu et al., 2021; Cao et al., 2021). Notably, N-linked glycan chains build a glycan shield, which masks the antigenic and neutralization epitopes on the GPC and thus facilitates the immune evasion of LASV (Watanabe et al., 2018; Koma et al., 2021; Sommerstein et al., 2015; Enriquez et al., 2022). The absence of N390 and N395 glycans was reported to promote the neutralization of neutralizing antibodies (Hastie et al., 2019).

We studied the effects of N-linked glycans on LASV GPC cleavage, infectivity, and the immune response (Zhu et al., 2021). In the present study, we examined the effects of glycosylation deficiency on membrane

* Corresponding author.
E-mail address: wangwei@wh.iov.cn (W. Wang).
[1] Siqi Dong and Wenting Mao contributed equally to this work.

https://doi.org/10.1016/j.virs.2023.04.003
Received 11 January 2023; Accepted 10 April 2023
Available online 12 April 2023

fusion. Intriguingly, deletion of the first glycan chain (N79Q) led to an increase in membrane fusion, unlike most previous reports in which deletion of the glycan chain led to a decrease in membrane fusion (Dash et al., 1994; Eichler et al., 2006; Sommerstein et al., 2015). The exploration of the biological functions of the LASV GPC N79 glycosylation site in this study helps us understand the infection mechanism of LASV and provides design strategies for attenuated vaccines for the treatment or prevention of LASV infection.

2. Materials and methods

2.1. Cells, plasmids, and virus

HEK293T, A549, and Vero E6 cells were cultured in Dulbecco's modified Eagle's medium (HyClone, Logan, UT, USA) supplemented with 10% fetal bovine serum (FBS; Gibco, Grand Island, NY, USA). To generate individual glycan deletion mutants, we introduced an asparagine-to-glutamine mutation into 11 N-glycosylation motifs (synthesized by Sangon, Shanghai, China) (Zhu et al., 2021). The pseudotype VSV (LASVpv, with single-cycle infection), bearing the GPC of LASV (strain Josiah, GenBank accession number HQ688673.1), and containing the Renilla luciferase (Rluc) reporter gene was generated as previously reported with a titer of 3×10^7/mL, and the recombinant virus (LASVrv, with multiple-cycle infection) containing the *GFP* gene was tittered as 1.6×10^7/mL (Wang et al., 2018). The genome copies of the pseudotyped viruses were quantified using qPCR, and Vero cells were infected with wild type (WT) and mutant pseudotyped viruses with the same genome copies.

2.2. Membrane fusion assay

For qualitative analysis, HEK293T were co-transfected with the plasmid pCAGGS-GPC containing each individual N-glycosylation mutant and pEGFP-N1. Twenty-four hours after transfection, the cells were exposed to the indicated pH of acidified medium for 10 min. The cells were then returned to neutral medium, and syncytium formation was observed 1 h later. Quantitative analysis was performed using ImageJ software, the average syncytia area was calculated using the analyzed particles, and the fusion index (FI) was calculated as follows: FI = average syncytia area at indicated pH/average syncytia area at pH 7.0. Confocal dynamic imaging was performed using an ANDOR Dragonfly 202 confocal microscope equipped with a 10× objective lens. Images were taken every 15 s and quantified using the ImageJ software.

For quantitative analysis, HEK293T cells, the effector cells in a 6-well plate, were transfected with 2.5 μg of pT7EMCVluc and 0.1 μg of pRL-CMV. The target HEK293T cells in a 24-well plate were transfected with 0.25 μg of pCAGGS-GPC and 0.25 μg of pCAGT7. Target cells were then overlaid with effector cells at a ratio of 1:1. The plasmids used in this assay were provided by Yoshiharu Matsuura (Osaka University, Osaka, Japan) (Aoki et al., 1998). After 12 h of co-culturing, the cells were exposed to the pH 5.0 acidified medium for 10 min and returned to neutral medium. Luciferase activity resulting from successful fusion was quantified 2 h later using a Dual-Glo Luciferase Assay (Promega, Madison, WI, USA). Cell fusion activity was determined using firefly luciferase (Fluc) activity and standardized with Rluc activity.

2.3. Western blotting

Proteins extracted from HEK293T cells were prepared using RIPA lysis buffer (Beyotime, Shanghai, China). Samples containing equal amounts of protein were separated using SDS-PAGE and then transferred to polyvinylidene difluoride (PVDF) membranes (Millipore, Burlington, MA, USA). The membrane was blocked with 5% skim milk in TBST for 1 h and then incubated overnight at 4 °C with the primary antibody against LASV-GP2 (diluted 1:1000), which was prepared by our group (Zhu et al., 2021). β-Tubulin Rabbit mAb (A12289, ABclonal, Wuhan, China; 1:1000) was used as a control for total proteins. Subsequently, the membranes were incubated with HRP Goat Anti-Rabbit IgG (H+L) (AS014, ABclonal; 1:5000) at room temperature for 45 min. The membranes were immersed in an enhanced chemiluminescence solution (Millipore) and the protein bands were detected using a ChemiDoc MP gel imager (Bio-Rad Laboratories, Hercules, CA, USA).

2.4. Cell surface biotinylation assay

HEK293T cells were transfected with pCAGGS-GPC WT or N79Q mutant. At 24 h post-transfection, cells were washed for three times with cold PBS at 4 °C and incubated with 10 mmol/L EZ-Link Sulfo-NHS-SS-Biotin buffer (Thermo Scientific, Waltham, MA, USA) for 30 min at room temperature to label the cell surface proteins. After biotinylation, the cells were washed for three times with cold PBS and lysed with Triton lysis buffer. Biotinylated cell surface proteins were collected using NeutrAvidin Beads (Thermo Scientific) and detected using Western blotting. The results are the mean of three independent determinations.

2.5. Binding assay

A549 cells were pretreated with 200 μg/mL monoclonal antibody IIH6 (sc-53987; Santa Cruz Biotechnology, Dallas, TX, USA) or IgM (sc-53347; Santa Cruz Biotechnology) control at 37 °C for 1 h. $LASVrv_{WT}$ and $LASVrv_{N79Q}$ (MOI = 1) were added and incubated at 4 °C for 1 h. The unbound virus particles were then washed for twice with cold PBS. After 18 h, cells were fixed with 4% paraformaldehyde and stained with DAPI. The GFP-positive and DAPI-positive cells were imaged using the Operetta High-Content Imaging System (PerkinElmer, USA), and the percentages of infected cells were calculated using Harmony 3.5 software. The results are the mean of three independent determinations.

2.6. Fusion inhibitor assay

Vero E6 cells were seeded at a density of 2.5×10^4 cells per well in 96-well plates. The Vero E6 cells were incubated with fusion inhibitors at the indicated concentration for 1 h, then infected with $LASVpv_{WT}$ or $LASVpv_{N79Q}$ (MOI = 0.1) for an additional 1 h. Twenty-three hours later, the cells were lysed, and luciferase activity was measured using the Rluc assay system (Promega).

2.7. Neutralization assay

Vero E6 cells were seeded at a density of 2.5×10^4 cells per well in 96-well plates. $LASVpv_{WT}$, $LASVpv_{N79Q}$, or combined mutations $LASVpv_{N79Q/N390Q}$ and $LASVpv_{N79Q/N395Q}$ (MOI = 1) were preincubated with the indicated concentrations of the 37.7H antibody at 37 °C for 1.5 h. Then, the virus-antibody mixtures were added to Vero E6 for 1 h. Cells were lysed 23 h later and luciferase activity was measured using the Rluc assay system (Promega, Madison, WI, USA).

2.8. One-step and multi-step growth curves

$LASVrv_{WT}$ and $LASVrv_{N79Q}$ were added to Vero E6 cells in 12-well plates at MOI = 2 for the one-step growth curve and MOI = 0.01 for the multi-step growth curve. One-hour post-infection, the inoculum was removed and the cell culture supernatant was collected every 12 h. Viral titers were determined using plaque assay.

2.9. Competitive growth assay

Vero E6 cells in 6-well plates were infected with the virus mixture at a total copy number of 1×10^6. The input mixture contained $LASVrv_{WT}$ and $LASVrv_{N79Q}$ at ratios of 1:1, 1:9, and 9:1, respectively. One-hour post-infection, the virus mixture was removed and replaced with a fresh medium. After an additional 24 h of incubation, the virus-

containing supernatants were collected and used to infect fresh Vero E6 cells. The viral RNAs from each passage were extracted, and cDNAs was synthesized using the HiScript II 1st Strand cDNA Synthesis Kit (Vazyme, Nanjing, China). LASV GPC was obtained using Easy Taq-PCR (TransGen, Beijing, China) and subjected to sequencing (Sanger, Shanghai, China).

3. Results

3.1. LASV GPC N79Q mutant promotes membrane fusion

Based on the similarity between amino acid structures, we used a strategy of mutating asparagine (N) to glutamine (Q) in the N-glycosylation motif to abolish the N-glycan chains linked to LASV GPC. Qualitative membrane fusion assays showed that the N89Q, N109Q, and N365Q mutants led to a sharp decrease in GPC-mediated membrane fusion. Interestingly, the N79Q mutant showed significantly enhanced membrane fusion, which was ~2.6 fold higher than that caused by the WT (Fig. 1A).

To test whether abolishing the first glycan chain (N79Q mutant) would change the pH threshold of membrane fusion, we examined the fusogenicity of both WT and N79Q at pH values from 4.5 to 7.0. As shown in Fig. 1B, neither WT nor N79Q could lead to membrane fusion at pH ≥ 5.5; N79Q resulted in apparent syncytium formation at pH = 5.0, whereas WT produced little syncytium, and both WT and N79Q led to total membrane fusion at pH = 4.5. These results demonstrate that N79Q increases the acid sensitivity of GPC-mediated membrane fusion, indicating that N79Q undergoes conformational change at a relatively higher pH. The quantitative fusion assay was then carried out at pH 5.0, and the results were in line with the qualitative assay that N79Q led to more syncytium formation than WT (Fig. 1C).

To further investigate the effects of the N79Q mutant on the dynamic process of membrane fusion, confocal live cell imaging was used to record the time-lapse video of membrane fusion. As shown in Fig. 1D and E, N79Q resulted in significant membrane fusion and complete loss of cell boundaries starting from 10 min after acid treatment. In contrast to N79Q, the WT produced only slight membrane fusion from 25 min after acid treatment (Supplementary Movies S1 and S2). The above results demonstrate that mutations promote membrane fusion by raising the pH threshold to trigger or delete the process of membrane fusion.

Supplementary video related to this article can be found at https://doi.org/10.1016/j.virs.2023.04.003

Since the first glycosylation site is conserved in the OW mammarenavirus (Sommerstein et al., 2015; Wang et al., 2016), we further examined whether mutations in the first glycosylation site would also have a facilitative effect on membrane fusion in other OW mammarenavirus. Notably, the promotion of membrane fusion was only observed in the LASV mutant, whereas it was absent in the LCMV and MOPV mutants (Fig. 1F).

3.2. N79Q mutation does not affect GPC expression and processing

N-glycans are essential for the expression, folding, and cleavage of viral glycoproteins (Watanabe et al., 2019). To investigate whether the N79Q mutation affects GPC expression and processing, we transfected HEK293T cells with pCAGGS-LASV-GPC$_{WT}$ and pCAGGS-LASV-GPC$_{N79Q}$, and detected the expression and processing of GPC. As shown in Fig. 2A–C, the N79Q mutant did not affect GPC expression or cleavage.

To investigate the effect of N79Q mutation on the extracellular trafficking of GPC, we used a biotinylation approach to detect the surface expression of N79Q. Transfected HEK293T cells were labeled with biotin and lysed for Western blotting, as described in Materials and methods. As shown in Fig. 2D and E, the surface transport of N79Q was similar to that of WT. These data indicate that the N79Q mutation does not affect GPC expression, cleavage, or cell-surface transport.

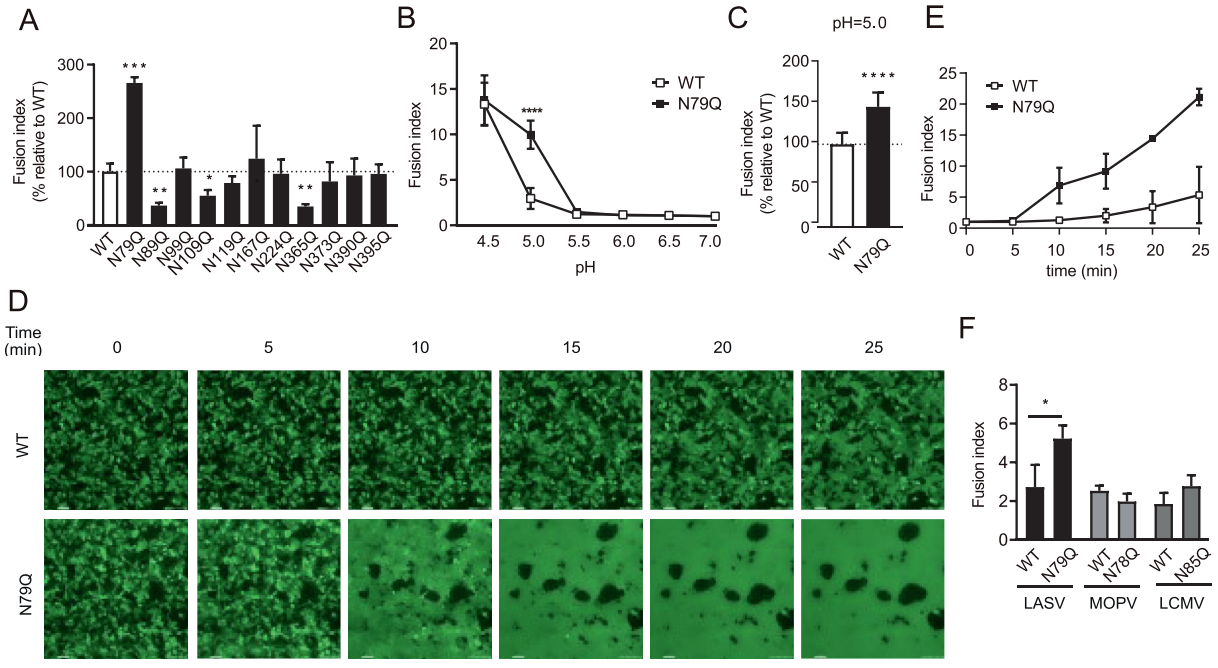

Fig. 1. Membrane fusion activity of N79Q mutant. **A** Membrane fusion screening of 11 N-glycosylation sites on LASV GPC. **B** WT GPC and N79Q GPC fusion activities at different pH. The HEK293T cells, co-transfected with pEGFP-N1 and WT GPC or N79Q GPC, were treated with acidified buffer (pH 4.5 to 7.0) for 10 min. Syncytium formation was visualized 1 h later and quantitated using ImageJ software. **C** The fusion activity was quantitatively determined by using the Dual-Glo luciferase assay. **D**, **E** Live-cell imaging of membrane fusion of N79Q and WT. (Supplementary Movies S1 and S2 in Supplementary Data); scale bars: 50 μm (**D**). The quantitative analysis was performed using ImageJ software (**E**). **F** Effects of corresponding mutations in other mammarenavirus. HEK 293T cells were transfected with LASV WT GPC, LASV N79Q GPC, LCMV WT GPC, LCMV N85Q GPC, MOPV WT GPC, and MOPV N78Q GPC. Fusion index (FI) = average syncytia area at indicated pH/average syncytia area at pH 7.0. Data are presented as means ± standard deviation from at least three independent experiments. The statistical significance was calculated by *t*-test. ****$P < 0.0001$, ***$P < 0.001$, **$P < 0.01$, *$P < 0.05$.

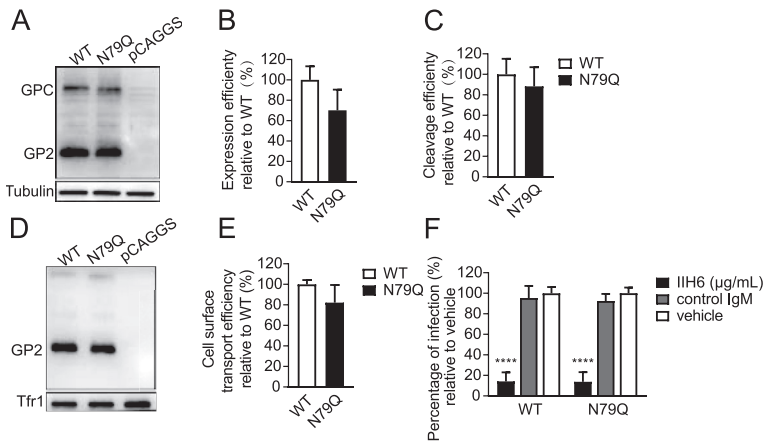

Fig. 2. Proteolytic processing and receptor binding of N79Q mutant. **A–C** Proteolytic processing of WT and N79Q GPC. The HEK293T cells transfected with pCAGGS-WT and pCAGGS-N79Q were subjected to Western blot (**A**), and quantitative analysis of the expression efficiency (**B**) and cleavage efficiency (**C**) were based on the protein bands. Efficiency was calculated as [(Volumn$_{N79Q}$ − Volumn$_{Background}$)/(Volumn$_{WT}$ − Volumn$_{Background}$) × 100%)]. **D, E** Surface transport of WT and N79Q GPC. The biotinylated cell surface proteins were subjected to Western blot (**D**), and quantitative analysis were conducted based on the protein bands (**E**). **F** Effect of N79Q mutant on GPC receptor binding. Data are presented as means ± standard deviation from three independent experiments. The statistical significance was calculated by *t*-test. ****$P < 0.0001$.

3.3. N79Q retained α-dystroglycan (α-DG) binding ability

LASV entry depends on binding of GP1 to the cell surface receptor α-DG (Cao et al., 1998). Deletion of the N79 glycan located in GP1 may affect virus-binding ability. Therefore, we pre-incubated A549 cells with the anti-α-DG monoclonal antibody IIH6 or negative control IgM, followed by infection with LASVrv$_{WT}$ and LASVrv$_{N79Q}$ (MOI = 1).

As shown in Fig. 2F, the infection rates of LASVrv$_{WT}$ and LASVrv$_{N79Q}$ in the IgM group were similar to those in the vehicle group; whereas the average infection rates of LASVrv$_{WT}$ and LASVrv$_{N79Q}$ in the IIH6 group were 14.17% and 13.79%, respectively. This showed that IIH6 could effectively inhibit infection by the recombinant virus, indicating that the N79Q mutation does not affect viral entry utilizing α-DG as an entry receptor.

3.4. LASVpv$_{N79Q}$ remained sensitive to membrane fusion inhibitors

It has been reported that some key mutants located in the transmembrane domain (TM) of GPC will confer the resistance to the membrane fusion inhibitor (Liu et al., 2021; Wang et al., 2018; Larson et al., 2008). To this end, we investigated whether GPC$_{N79Q}$ is resistant to membrane fusion inhibitors such as ST-193, casticin, and lacidipine, which have been reported to inhibit LASV entry by targeting the GPC TM, thus blocking GPC-mediated membrane fusion (Liu et al., 2021; Wang et al., 2018; Larson et al., 2008). As shown in Fig. 3, all three compounds exhibited dose-dependent inhibition of LASVpv$_{N79Q}$, and the inhibition was similar to that of the LASVpv$_{WT}$, indicating that the N79Q mutant remained sensitive to membrane fusion inhibitors.

3.5. Deletion of N79 glycan enhanced the recognition of GPC by neutralizing antibody 37.7H

The neutralizing antibody 37.7H, isolated from the survivor of Lassa fever, specifically binds two monomers, and stabilizes the GPC trimer conformation to prevent membrane fusion (Hastie et al., 2017). The 37.7H identified the major neutralizing epitope GPC-B masked by the tenth and eleventh glycan chains, and the distal mannose of the N79 glycan chain would contact the light chain of 37.7H (Hastie et al., 2019; Watanabe et al., 2018; Robinson et al., 2016). To investigate whether the absence of the first glycan chain would weaken the binding of the antibody to GPC, the neutralization effect of 37.7H on LASVpv$_{N79Q}$ was studied. As shown in Fig. 4A, LASVpv$_{N79Q}$ was more sensitive to 37.7H at the higher tested concentrations ranging from 4 to 16 nmol/L, suggesting that the deletion of the first glycan chain may expose part of the epitope recognized by 37.7H. To this end, we further explored whether the first glycan chain has a synergistic effect with the tenth and eleventh glycan chains (N390 and N395) on the enhancement of 37.7H recognition. As shown in Fig. 4B and C, deletion of either the tenth (N390Q) or eleventh (N395Q) glycan chain alone enhanced the suppressive effect of 37.7H on pseudoviruses, whereas combining the first and tenth glycosylation

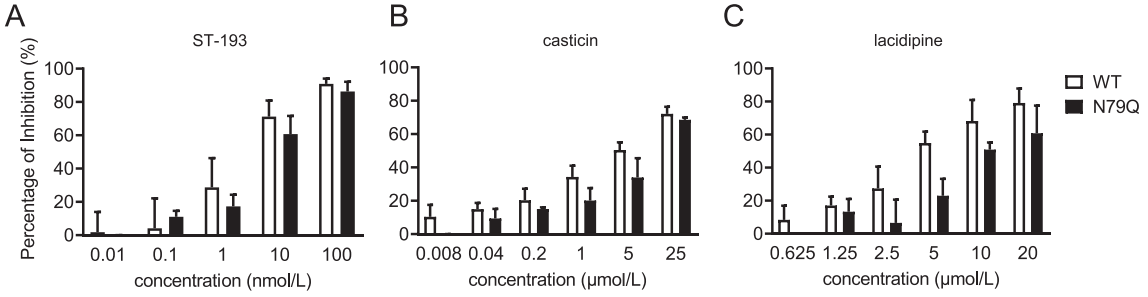

Fig. 3. The effects of fusion inhibitors on LASVpv$_{N79Q}$ infection. The Vero E6 cells were incubated with fusion inhibitors ST-193 (**A**), casticin (**B**), and lacidipine (**C**) at the indicated concentration for 1 h, then cells were infected with pseudotype LASVpv$_{WT}$ and LASVpv$_{N79Q}$ (MOI = 0.1), respectively, for an additional 1 h. Twenty-three hours later, the cells were lysed, and luciferase activity was measured using the Rluc assay system. Inhibition was calculated as (Rluc$_{Drug}$/Rluc$_{DMSO}$ × 100%). Data are presented as means ± standard deviation from 4 to 5 independent experiments.

deletion mutations, or combining the first and eleventh glycosylation deletion mutations, resulted in a more significant suppressive effect than N79Q mutation alone (Fig. 4D), indicating that the glycan chain plays an important role in masking neutralizing epitopes and antibody recognition.

3.6. N79Q attenuates the virulence of recombinant LASV

Given the critical role of membrane fusion in the life cycle of LASV, we investigated the effect of the N79Q mutant on the viral life cycle. First, the recombinant viruses with complete life cycles, named LASVrv$_{WT}$ and LASVrv$_{N79Q}$, were rescued as previously reported (Hou et al., 2022; Wang et al., 2018). As shown in single-step growth curves and multi-step growth curves (Fig. 5A and B), LASVrv$_{N79Q}$ consistently grew slower than LASVrv$_{WT}$ and took a longer time to reach the plateau stage, indicating that the first glycosylation site mutation attenuated the virulence of recombinant LASV. Furthermore, by performing sequential passages of a mixture of LASVrv$_{N79Q}$ and LASVrv$_{WT}$ in different ratios, we found that LASVrv$_{WT}$ completely replaced LASVrv$_{N79Q}$ after one round of passages in an equal-ratio mixture. Interestingly, even in the case of the 1:9 mixture of WT and N79Q, WT replaced N79Q after only two rounds of passage (Fig. 5C). Notably, LASVrv$_{N79Q}$ alone was very stable in successive passages, with no spurious peaks in successive passages, even after 15 rounds.

4. Discussion

LASV GPC is a highly glycosylated glycoprotein with 11 N-linked glycosylation sites that are evenly distributed on the surface of the viral particles and obscure the antigenic epitopes on the GPC. In this study, we found that mutation of the first glycosylation site, N79Q, promoted GPC-mediated membrane fusion. In addition, we also used other mutations N79A and T81A that disrupt the first glycosylation motif, again confirming that deletion of the first glycosylation site increases membrane fusion (Supplementary Fig. S1). In general, mutations that lead to the structural deletion of proteins are often accompanied by impairment of protein function. Intriguingly, the N79Q mutation resulted in the deletion of the glycan chain, which not only enhanced but also promoted GPC-mediated membrane fusion. We hypothesized that this site was more biologically important; therefore, we conducted a follow-up study on the other biological functions of the N79 glycosylation site.

The correct expression and processing of GPC are the basis of GPC functions such as membrane fusion. The N79Q mutant did not affect GPC expression, processing, or cell membrane surface transport. Based on the reported protein structure of LASV GPC (Katz et al., 2022), it was found that the first glycan chain might interact with the W283 site on the GPC to obscure the fusion peptide located in GP2, which functions to maintain the stability of the highly hydrophobic region (Fig. 6). Deletion of the first glycan of the N79Q mutation leads to the exposure of fusion peptide, thus loosening the structure of GP2 and making it more susceptible to the fusion conformation transition under low pH induction. We are currently trying to use S2 cells to express the extracellular domain of GPC and hope to further elucidate the potential mechanism of the LASV GPC N79Q pro-fusion phenotype through biochemical assays.

The glycosylation sites N390 and N395 are located directly on the neutralizing epitope of 37.7H, and the glycan chains on them have a direct interference effect on the recognition of neutralizing antibody 37.7H (Robinson et al., 2016). The glycosylation site N79 is in the vicinity of the 37.7H neutralizing epitope. In this study, we found that the N79Q mutation enhances the neutralization effect of 37.7H on pseudovirus infection. However, regarding our combined mutant GPC N79Q/N390Q or N79Q/N395Q, we found that the N79Q mutation was not synergistic in enhancing the recognition of 37.7H compared to N390Q and N395Q mutations alone. Intriguingly, the N79Q mutant strain was significantly less virulent than the WT strain. N79Q promoted GPC-mediated membrane fusion but impaired virulence. There are three speculations about this phenomenon: (1) the N79Q mutation leads to a structural defect and the loose structure of GPC is not conducive to viral infection and proliferation. (2) The pro-membrane fusion phenotype may prematurely release the viral genome into the cytoplasm, leading to a reduction in the expression and replication of the viral genome. (3) N79Q mutations may lead to reduced virulence of the virus by affecting other processes in the viral life cycle, such as viral particle assembly and germination.

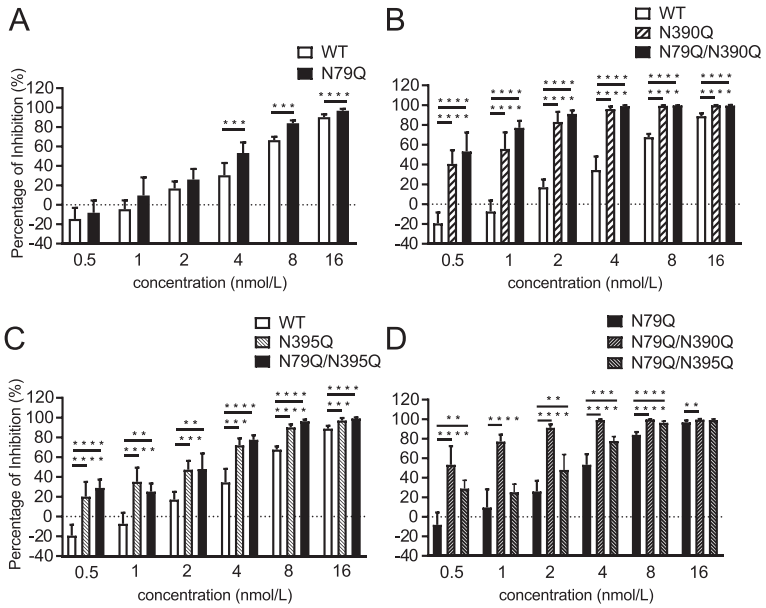

Fig. 4. The effect of N79Q mutant on the sensitivity of pseudotype LASVpv to the neutralization antibody 37.7H. LASVpv$_{WT}$, LASVpv$_{N79Q}$, LASVpv$_{N79Q/N390Q}$, and LASVpv$_{N79Q/N395Q}$ (MOI = 1) were pre-incubated with 37.7H antibody at 37 °C for 1.5 h, respectively; and then added to the Vero E6 cells for an additional 1 h incubation. The luciferase activity was tested 24 h later. Data are presented as means ± standard deviation from 4 to 6 independent experiments. The statistical significance was calculated by *t*-test. ****$P < 0.0001$; ***$P < 0.001$; **$P < 0.01$.

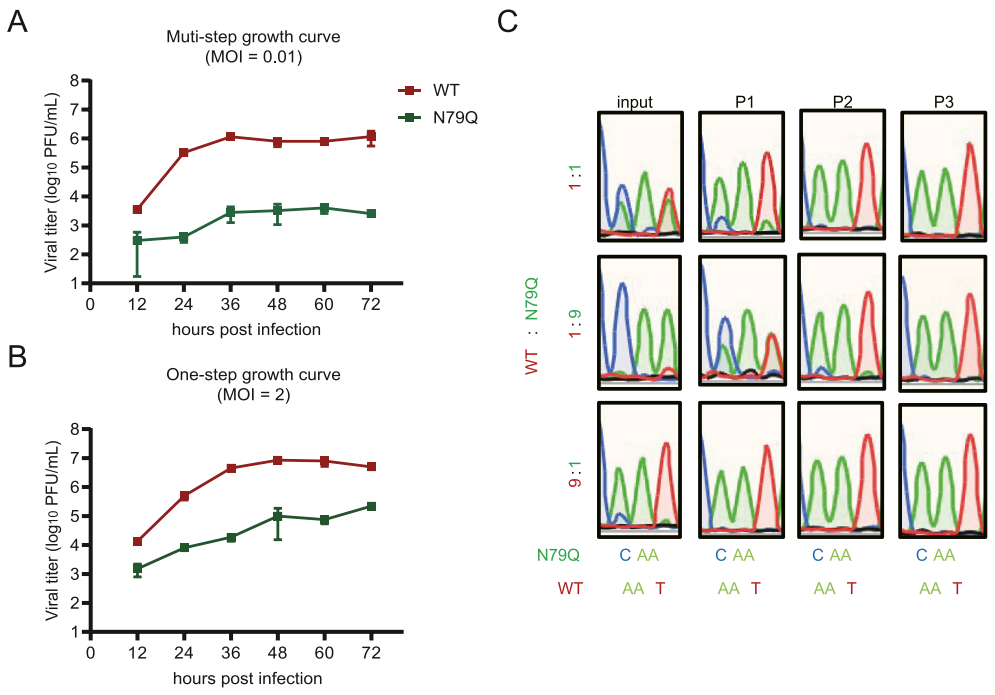

Fig. 5. Growth characteristics of N79Q mutant. Multi-step (**A**) and single-step (**B**) growth kinetics of recombinant LASVrv$_{WT}$ and LASVrv$_{N79Q}$. The supernatant was collected at the indicated times and subjected for plaque assay. Data are presented as means ± standard deviation from three independent experiments. **C** Coinfection competition of LASVrv$_{WT}$ and LASVrv$_{N79Q}$. Vero E6 cells were infected with a 1:1, 1:9, and 9:1 ratio of LASVrv$_{WT}$ and LASVrv$_{N79Q}$ at total genome copies of 1×10^6 in 1 mL. The RNA was extracted after every passaging, and subjected to Sanger sequencing for GPC.

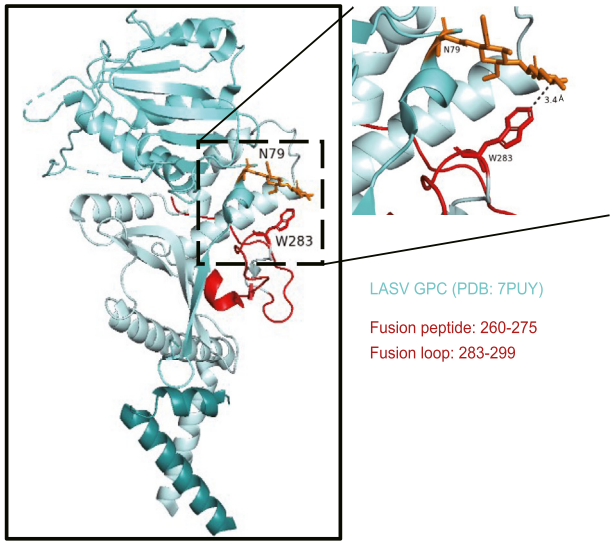

Fig. 6. The interaction between the first glycan chain and W283. Shown is the ribbon diagram view of monomer LASV GPC (cyan; PDB: 7PUY). The interactions between the first glycan chain (orange) and the side chain of W283 (red) were enlarged, and the fusion peptide and fusion loop were highlighted in red. The distance was predicted to be resolution 1.25 Å.

There is no licensed vaccine or drug against LASV, and there is an unmet need to develop anti-LASV drugs. Glycosylation of viral proteins plays an important role in multiple stages of the viral life cycle. Understanding the biological functions of key glycosylation sites on the GPC of LASV could help us better understand the mechanisms of LASV infection and provide a better understanding for the development of LASV-specific therapeutic and preventive drugs. In addition, identifying conserved glycosylation patterns is paramount to the development of efficient vaccines for highly diverse viruses (Sommerstein et al., 2015; Zhu et al., 2021). It is possible to generate a refocused B-cell response to the vaccine and improve the neutralization of homologous, heterologous and heterotypic viruses by mutating certain conserved glycans (Schön et al., 2020; Watanabe et al., 2019). Our study showed that deletion of N79 glycan attenuated virulence, which will provide design strategies for the development of live attenuated vaccines for the treatment or prevention of LASV infection.

5. Conclusions

In this study, we screened all the 11 glycan sites in LASV GPC, and found that ablation mutant of the first glycan would lead the promotion of the GPC-mediated membrane fusion. Subsequently, the role of the first glycan in the LASV GPC was extensively investigated, and these findings will be useful for vaccine and drug design.

Data availability

All the data generated during the current study are included in the manuscript.

Ethics statement

This article does not contain any studies with human or animal subjects performed by any of the authors.

Author contributions

Siqi Dong: conceptualization; data curation; formal analysis; investigation; methodology; software; validation; visualization; writing original draft; writing-review and editing. Wenting Mao: conceptualization; data curation; formal analysis; investigation; methodology; software; validation; visualization; writing-review and editing. Yang Liu: data curation;

investigation and methodology. Xiaoying Jia: investigation and methodology. Yueli Zhang: investigation and methodology. Minmin Zhou: investigation and methodology. Yuxia Hou: investigation and methodology. Gengfu Xiao: funding acquisition. Wei Wang: conceptualization; funding acquisition; methodology; project administration; resources; supervision; validation; writing-review and editing.

Conflict of interest

The authors declare that they have no conflicts of interest.

Acknowledgements

We thank the Center for Instrumental Analysis and Metrology, and Institutional Center for Shared Technologies and Facilities of Wuhan Institute of Virology, CAS for providing technical assistance. This work was supported by the National Key Research and Development Program (2022YFC2303300, 2018YFA0507204), the Strategic Priority Research Program of the Chinese Academy of Sciences (XDB0490000), the National Natural Science Foundation of China (82172273, 31670165).

Appendix A. Supplementary data

Supplementary data to this article can be found online at https://doi.org/10.1016/j.virs.2023.04.003.

References

Aoki, Y., Aizaki, H., Shimoike, T., Tani, H., Ishii, K., Saito, I., Matsuura, Y., Miyamura, T., 1998. A human liver cell line exhibits efficient translation of HCV RNAs produced by a recombinant adenovirus expressing T7 RNA polymerase. Virology 250, 140–150.

Cao, J., Zhang, G., Zhou, M., Liu, Y., Xiao, G., Wang, W., 2021. Characterizing the Lassa virus envelope glycoprotein membrane proximal external region for its role in fusogenicity. Virol. Sin. 36, 273–280.

Cao, W., Henry, M.D., Borrow, P., Yamada, H., Elder, J.H., Ravkov, E.V., Nichol, S.T., Compans, R.W., Campbell, K.P., Oldstone, M.B., 1998. Identification of alpha-dystroglycan as a receptor for lymphocytic choriomeningitis virus and Lassa fever virus. Science 282, 2079–2081.

Dash, B., Mcintosh, A., Barrett, W., Daniels, R., 1994. Deletion of a single N-linked glycosylation site from the transmembrane envelope protein of human immunodeficiency virus type 1 stops cleavage and transport of gp160 preventing env-mediated fusion. J. Gen. Virol. 75, 1389–1397.

Eichler, R., Lenz, O., Garten, W., Strecker, T., 2006. The role of single N-glycans in proteolytic processing and cell surface transport of the Lassa virus glycoprotein GP-C. Virol. J. 3, 41.

Eichler, R., Lenz, O., Strecker, T., Eickmann, M., Klenk, H.D., Garten, W., 2003. Identification of Lassa virus glycoprotein signal peptide as a trans-acting maturation factor. EMBO Rep. 4, 1084–1088.

Enriquez, A.S., Buck, T.K., Li, H., Norris, M.J., Moon-Walker, A., Zandonatti, M.A., Harkins, S.S., Robinson, J.E., Branco, L.M., Garry, R.F., Saphire, E.O., Hastie, K.M., 2022. Delineating the mechanism of anti-Lassa virus GPC-A neutralizing antibodies. Cell Rep. 39, 110841.

Hastie, K.M., Cross, R.W., Harkins, S.S., Zandonatti, M.A., Koval, A.P., Heinrich, M.L., Rowland, M.M., Robinson, J.E., Geisbert, T.W., Garry, R.F., Branco, L.M., Saphire, E.O., 2019. Convergent structures illuminate features for germline antibody binding and pan-lassa virus neutralization. Cell 178, 1004–1015 e14.

Hastie, K.M., Zandonatti, M.A., Kleinfelter, L.M., Heinrich, M.L., Rowland, M.M., Chandran, K., Branco, L.M., Robinson, J.E., Garry, R.F., Saphire, E.O., 2017. Structural basis for antibody-mediated neutralization of Lassa virus. Science 356, 923–928.

Hou, Y., Liu, Y., Jia, X., Zhou, M., Mao, W., Dong, S., Zhang, Y., Xiao, G., Wang, W., 2022. Screening and identification of lassa virus entry inhibitors from a fragment-based drug discovery library. Viruses 14, 2649.

Houlihan, C., Behrens, R., 2017. Lassa fever. BMJ 358, j2986.

Katz, M., Weinstein, J., Eilon-Ashkenazy, M., Gehring, K., Cohen-Dvashi, H., Elad, N., Fleishman, S.J., Diskin, R., 2022. Structure and receptor recognition by the Lassa virus spike complex. Nature 603, 174–179.

Koma, T., Huang, C., Coscia, A., Hallam, S., Manning, J.T., Maruyama, J., Walker, A.G., Miller, M., Smith, J.N., Patterson, M., Abraham, J., Paessler, S., 2021. Glycoprotein N-linked glycans play a critical role in arenavirus pathogenicity. PLoS Pathog. 17, e1009356.

Kuhn, J.H., Adkins, S., Agwanda, B.R., AL Kubrusli, R., Alkhovsky, S.V., Amarasinghe, G.K., Avsic-Zupanc, T., Ayllon, M.A., Bahl, J., Balkema-Buschmann, A., Ballinger, M.J., Basler, C.F., Bavari, S., Beer, M., Bejerman, N., Bennett, A.J., Bente, D.A., Bergeron, E., Bird, B.H., Blair, C.D., Blasdell, K.R., Blystad, D.R., Bojko, J., Borth, W.B., Bradfute, S., Breyta, R., Briese, T., Brown, P.A., Brown, J.K., Buchholz, U.J., Buchmeier, M.J., Bukreyev, A., Burt, F., Buttner, C., Calisher, C.H., Cao, M., Casas, I., Chandran, K., Charrel, R.N., Cheng, Q., Chiaki, Y., Chiapello, M., Choi, I.R., Ciuffo, M., Clegg, J.C.S., Crozier, I., Dal Bo, E., DE LA Torre, J.C., DE Lamballerie, X., DE Swart, R.L., Debat, H., Dheilly, N.M., DI Cicco, E., DI Paola, N., DI Serio, F., Dietzgen, R.G., Digiaro, M., Dolnik, O., Drebot, M.A., Drexler, J.F., Dundon, W.G., Duprex, W.P., Durrwald, R., Dye, J.M., Easton, A.J., Ebihara, H., Elbeaino, T., Ergunay, K., Ferguson, H.W., Fooks, A.R., Forgia, M., Formenty, P.B.H., Franova, J., Freitas-Astua, J., Fu, J., Furl, S., Gago-Zachert, S., Gao, G.F., Garcia, M.L., Garcia-Sastre, A., Garrison, A.R., Gaskin, T., Gonzalez, J.J., Griffiths, A., Goldberg, T.L., Groschup, M.H., Gunther, S., Hall, R.A., Hammond, J., Han, T., Hepojoki, J., Hewson, R., Hong, J., Hong, N., Hongo, S., Horie, M., Hu, J.S., Hu, T., Hughes, H.R., Huttner, F., et al., 2021. 2021 Taxonomic update of phylum negarnaviricota (riboviria: orthornavirae), including the large orders bunyavirales and mononegavirales. Arch. Virol. 166, 3513–3566.

Larson, R.A., Dai, D., Hosack, V.T., Tan, Y., Bolken, T.C., Hruby, D.E., Amberg, S.M., 2008. Identification of a broad-spectrum arenavirus entry inhibitor. J. Virol. 82, 10768–10775.

Lenz, O., Ter Meulen, J., Klenk, H.D., Seidah, N.G., Garten, W., 2001. The Lassa virus glycoprotein precursor GP-C is proteolytically processed by subtilase SKI-1/S1P. Proc. Natl. Acad. Sci. U. S. A. 98, 12701–12705.

Liu, Y., Guo, J., Cao, J., Zhang, G., Jia, X., Wang, P., Xiao, G., Wang, W., 2021. Screening of botanical drugs against lassa virus entry. J. Virol. 95, e02429-20.

Lo Iacono, G., Cunningham, A.A., Fichet-Calvet, E., Garry, R.F., Grant, D.S., Khan, S.H., Leach, M., Moses, L.M., Schieffelin, J.S., Shaffer, J.G., Webb, C.T., Wood, J.L., 2015. Using modelling to disentangle the relative contributions of zoonotic and anthroponotic transmission: the case of lassa fever. PLoS Neglected Trop. Dis. 9, e3398.

Lukashevich, I.S., Torre, J.C., 2021. Special issue “Arenaviruses 2020”. Viruses 13, 703.

Mccormick, J.B., Webb, P.A., Krebs, J.W., Johnson, K.M., Smith, E.S., 1987. A prospective study of the epidemiology and ecology of Lassa fever. J. Infect. Dis. 155, 437–444.

Nunberg, J.H., York, J., 2012. The curious case of arenavirus entry, and its inhibition. Viruses 4, 83–101.

Robinson, J.E., Hastie, K.M., Cross, R.W., Yenni, R.E., Elliott, D.H., Rouelle, J.A., Kannadka, C.B., Smira, A.A., Garry, C.E., Bradley, B.T., Yu, H., Shaffer, J.G., Boisen, M.L., Hartnett, J.N., Zandonatti, M.A., Rowland, M.M., Heinrich, M.L., Martinez-Sobrido, L., Cheng, B., DE LA Torre, J.C., Andersen, K.G., Goba, A., Momoh, M., Fullah, M., Gbakie, M., Kanneh, L., Koroma, V.J., Fonnie, R., Jalloh, S.C., Kargbo, B., Vandi, M.A., Gbetuwa, M., Ikponmwosa, O., Asogun, D.A., Okokhere, P.O., Follarin, O.A., Schieffelin, J.S., Pitts, K.R., Geisbert, J.B., Kulakoski, P.C., Wilson, R.B., Happi, C.T., Sabeti, P.C., Gevao, S.M., Khan, S.H., Grant, D.S., Geisbert, T.W., Saphire, E.O., Branco, L.M., Garry, R.F., 2016. Most neutralizing human monoclonal antibodies target novel epitopes requiring both Lassa virus glycoprotein subunits. Nat. Commun. 7, 11544.

SchöN, K., Lepenies, B., Goyette-Desjardins, G., 2020. Impact of protein glycosylation on the design of viral vaccines. Adv. Biochem. Eng. Biotechnol. 175, 319–354.

Sommerstein, R., Flatz, L., Remy, M.M., Malinge, P., Magistrelli, G., Fischer, N., Sahin, M., Bergthaler, A., Igonet, S., Ter Meulen, J., Rigo, D., Meda, P., Rabah, N., Coutard, B., Bowden, T.A., Lambert, P.H., Siegrist, C.A., Pinschewer, D.D., 2015. Arenavirus glycan shield promotes neutralizing antibody evasion and protracted infection. PLoS Pathog. 11, e1005276.

Wang, P., Liu, Y., Zhang, G., Wang, S., Guo, J., Cao, J., Jia, X., Zhang, L., Xiao, G., Wang, W., 2018. Screening and identification of lassa virus entry inhibitors from an FDA-approved drug library. J. Virol. 92, e00954-18.

Wang, W., Zhou, Z., Zhang, L., Wang, S., Xiao, G., 2016. Structure-function relationship of the mammarenavirus envelope glycoprotein. Virol. Sin. 31, 380–394.

Watanabe, Y., Bowden, T.A., Wilson, I.A., Crispin, M., 2019. Exploitation of glycosylation in enveloped virus pathobiology. Biochim. Biophys. Acta Gen. Subj. 1863, 1480–1497.

Watanabe, Y., Raghwani, J., Allen, J.D., Seabright, G.E., Li, S., Moser, F., Huiskonen, J.T., Strecker, T., Bowden, T.A., Crispin, M., 2018. Structure of the Lassa virus glycan shield provides a model for immunological resistance. Proc. Natl. Acad. Sci. U. S. A. 115, 7320–7325.

Zhu, X., Liu, Y., Guo, J., Cao, J., Wang, Z., Xiao, G., Wang, W., 2021. Effects of N-linked glycan on lassa virus envelope glycoprotein cleavage, infectivity, and immune response. Virol. Sin. 36, 774–783.